A stochastic collocation approach for efficient integrated gear health prognosis

Fuqiong Zhao[a], Zhigang Tian[b,*], Yong Zeng[b]

[a]*Department of Mechanical and Industrial Engineering, Concordia University, 1515 ste-catherine street, west, Montreal, Quebec, Canada H3G 2W1*

[b]*Concordia Institute for Information Systems Engineering, Concordia University, 1515 Ste-Catherine Street, West EV-7.637, Montreal, Quebec, Canada H3G 2W1*

Abstract - Uncertainty quantification in damage growth is critical in equipment health prognosis and condition based maintenance. Integrated health prognostics has recently drawn growing attention due to its capability to produce more accurate predictions through integrating physical models and real-time condition monitoring data. In the existing literature, simulation is commonly used to account for the uncertainty in prognostics, which is inefficient. In this paper, instead of using simulation, a stochastic collocation approach is developed for efficient integrated gear health prognosis. Based on generalized polynomial chaos expansion, the approach is utilized to evaluate the uncertainty in gear remaining useful life prediction as well as the likelihood function in Bayesian inference. The collected condition monitoring data is incorporated into prognostics via Bayesian inference to update the distributions of uncertainties at certain inspection times. Accordingly, the distribution of the remaining useful life is updated. Comparing to conventional simulation methods, the stochastic collocation approach is much more efficient, and is capable of dealing with high dimensional probability space. An example is used to demonstrate the effectiveness and efficiency of the proposed approach.

Key Words – Integrated prognostics, Polynomial chaos expansion, Stochastic collocation, Gear, Bayesian inference, Remaining useful life prediction

* Z. Tian is with Concordia Institute for Information Systems Engineering, Concordia University. 1515 Ste-Catherine Street West EV-7.637, Montreal, QC H3G 2W1, Canada (e-mail: tian@ciise.concordia.ca).

1. Introduction

To maintain the reliability and performance of mechanical components and systems, condition based maintenance (CBM), including on-line diagnostics, prognostics and maintenance optimization, play a critical role [1,2,3]. Unexpected failures will cause unexpected downtime, which can interrupt normal production, delay commitment and undermine brand reputation. The objective of CBM is to optimize maintenance schedule for avoiding unexpected failures and reducing overall maintenance cost. Prediction of when the failure possibly arrives is an essential work in CBM and prognostics and health management (PHM). Health condition prediction is based on two components: one is the current condition carried by the sensor data, and the other is the prognostics model, being physical or data-driven. Gear is a basic component in transmission systems, such as those in automotive engines and helicopters. This paper focuses on the remaining useful life prediction of gears with crack at the tooth root due to cyclic loading.

Lots of research work has been done in health prognosis methods for damage propagation [4,5]. In those papers, the parameters appearing in the physical models are treated as constants. However, the fatigue degradation process is accompanied with various sources of uncertainties, which can result in failure time differences among different units. For example, due to material variation, experimental errors, measurement inaccuracy as well as variations of operating condition, failure time should take the form of statistical distribution rather than a single value. So the prognosis of equipment future condition or component failure time should be studied in a probabilistic framework. The quantification, propagation and updating of uncertainty are the main tasks in probabilistic prognostics. In the paper by Zhao et al. [6], an integrated gear prognosis method was developed by utilizing both gear physical models and real-time condition monitoring data in an integrated way. The integrated prognosis identified the distributions of the material and model uncertainties for the current specific unit being monitored by fusing the condition monitoring data using Bayesian inference.

Monte Carlo (MC) simulation and its variants are the commonly used tools to account for these uncertainty factors. Kacprzynski et al. [7] presented a gear prognosis tool using 3D gear finite element modeling and considered various uncertainty factors in damage propagation, while the condition monitoring information was used to estimate the current crack length with uncertainty. Coppe et al. [8] used MC simulation to calculate the proposed likelihood function to

update the distribution of material parameters. The two parameters were considered separately, which means only one uncertainty factor was considered when using MC simulation. In the paper by Sankararaman et al. [9], the global sensitivity analysis was applied in order to select only a few effective uncertain parameters, e.g., three parameters were selected in the numerical example, among all the possible parameters for calibration. The main reason is that the multi-dimensional calibration procedure is computationally intensive using MC analysis. Typically a large number of executions of deterministic problem solving are needed as MC solution converges relative slowly. Furthermore, for a complex system where the solution of a single deterministic realization is very time-consuming, MC becomes impractical due to prohibitive computation time.

Generalized polynomial chaos (gPC) is a method to analyze and quantify the effect of random input parameters in the process governed by the ordinary/partial differential equations. Built on a rigorous mathematics theory, gPC has several preferable merits in dealing with uncertainty quantification which makes this technique significantly attractive. With gPC, the numerical stochastic solution could be expressed as the expansion of orthogonal polynomials which are functions of the random input variables. gPC expansion is essentially a spectral representation in random space, and exhibits fast convergence when the expanded function depends smoothly on the random parameters [10]. By selecting the optimal type of orthogonal polynomial, the convergence rate could become exponential if the function is analytic, i.e., infinitely smooth [11].

A large number of research papers have been published, presenting the computational efficiency and accuracy provided by gPC technique in many fields, most of which are nonlinear problems with high dimensional uncertainties, e.g. fluid dynamics [12-14, 21-22], chemistry reaction [15], solid mechanics [16-17], etc. For highly-nonlinear problem, a sufficiently high order polynomial space is required, as reported in Ref. [18-19].

The quantities to be solved in gPC are those coefficients of the polynomial expansion. There are two basic methods to calculate them: stochastic Galerkin (SG) method and stochastic collocation (SC) method. SG method is well developed to solve the stochastic problems. Reagan et al. [20] and Najm et al. [15] investigated uncertainty quantification in chemical systems using SG method. In computational fluid dynamics, SG method has many applications as well [21,22]. However, SG method reformulates the stochastic problem into a larger coupled set of equations

of coefficients, and thus the computational work is still cumbersome. Furthermore, when the original problem takes highly complex and nonlinear form, the derivation of the gPC Galerkin model can be nontrivial, sometimes impossible. Due to these limitations of SG method, there has been a growing interest in another class of method known as SC method. SC method has the power to take advantage of both SG method and MC method to achieve high resolution from polynomial approximations in random spaces with the ease of implementation [23]. It is widely acknowledged that SC based gPC collaborated with sparse grid has appealing capability in handling high-dimensional random spaces. With the dimension increases, sparse grid algorithm is able to mitigate "curse of dimensionality" to a large degree, and meanwhile maintain the numerical integration accuracy inherited from 1D integration rule as much as possible. A numerical algorithm based on SC for establishing the dependency of observables on random parameters was proposed by Xiu [10]. gPC also serves as an efficient way to solve Bayesian inference problem where the likelihood function was defined as the Gaussian measurement error [24]. In the present paper, we aim to develop an efficient integrated approach for gear health prognosis based on gPC SC method.

In this paper, based on the integrated prognostics framework proposed in [6], a stochastic collocation approach is developed for efficient integrated gear health prognosis. Instead of using simulation, stochastic collocation methods based on gPC are utilized to evaluate gear remaining useful life prediction uncertainty as well as the likelihood function in Bayesian inference. More specifically, in Bayesian inference, where the likelihood function is defined as function of not only Gaussian measurement error but also random model inputs, the stochastic collocation method is used to calculate the crack distribution with uncertainty induced by random model inputs. Furthermore, the stochastic collocation method is also used to calculate failure time distribution by dealing with uncertainty propagation through Paris' law. The uncertain parameters in Paris' law are modeled as random variables and the crack propagation process based on Paris' law is treated as stochastic. The failure time of a cracked gear is expressed as the summation of a series of orthogonal polynomials with random variables. Fig. 1 sketches the core structure of the proposed approach.

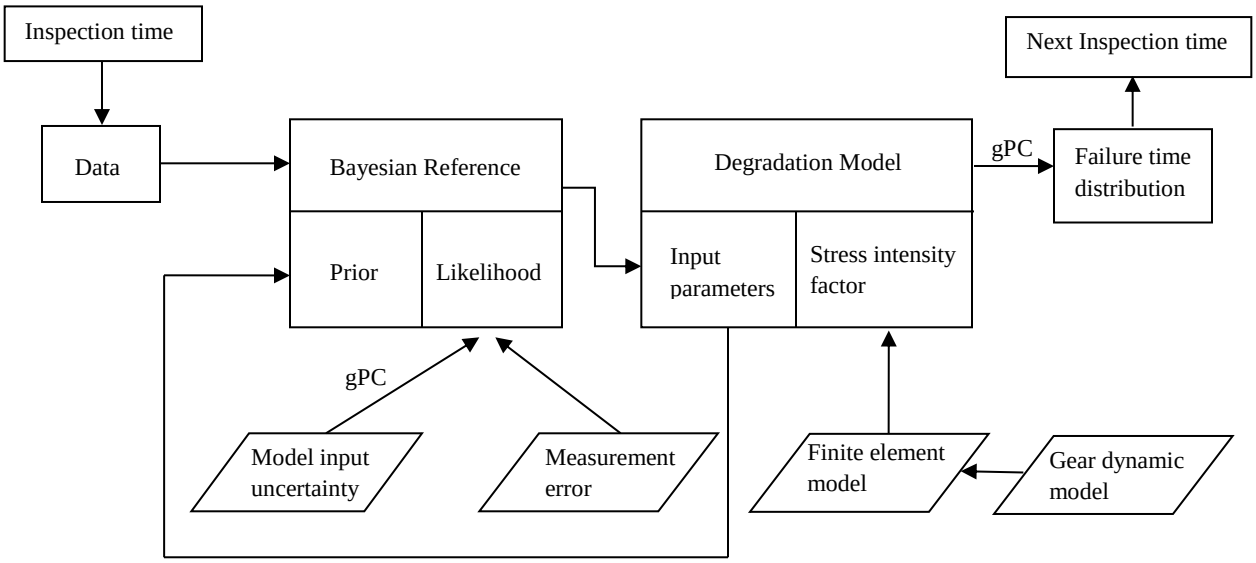

Fig.1. Structure of the proposed prognosis approach based on gPC stochastic collocation

The remainder of this paper is organized as follows. The fundamentals of generalized polynomial expansion and the stochastic collocation method are presented in Section 2. The framework of integrated gear prognosis method is briefly introduced in Section 3. The application of gPC stochastic collocation in the integrated gear prognosis framework is discussed in details in Section 4, which as well includes the elaborate explanation of Fig.1. Section 5 presents an example to demonstrate the efficiency and effectiveness of the proposed approach for uncertainty quantification. Conclusions are given in Section 6.

Abbreviations:

CBM: condition based maintenance

PHM: prognostics and health management

RUL: remaining useful life

gPC: generalized polynomial chaos

PCE: polynomial chaos expansion

SIF: stress intensity factor

FE: finite element

HPSTC: highest point of single tooth contact

2. Fundamentals of gPC stochastic collocation method

In this section, the fundamentals of gPC expansion and stochastic collocation method on sparse grid are briefly presented. The gPC expansion can be considered as an efficient approximation to stochastic processes and random variables. To introduce this technique and further investigate the approximation properties, a probability space, $(\Omega, \mathcal{F}, \mathcal{P})$, needs to be properly defined, where Ω is the event space, $\mathcal{F}$ is the σ-field of Ω, and $\mathcal{P}$ is a probability measure.

2.1 gPC expansion

Let $Y = (Y_1, \cdots, Y_d)$ be a d-variate random vector in the probability space $(\Omega, \mathcal{F}, \mathcal{P})$, with the cumulative distribution function $F_Y(y)$ and the support Γ_Y. Assume that the components $Y_1, \cdots, Y_d$ are mutually independently identical random variables, which implies $F_Y(y) = \prod_{i=1}^{d} F_{Y_i}(y_i)$.

Starting with one-dimensional case, let $\mathbb{P}_N(Y_i)$ be univariate polynomial space with degree up to N, and $\{\phi_k(Y_i), k = 0, \cdots, N\} \subset \mathbb{P}_N(Y_i)$. We call $\{\phi_k(Y_i), k = 0, \cdots, N\}$ univariate gPC basis functions in $\mathbb{P}_N(Y_i)$ if they satisfy the following orthogonality condition

$$\mathbb{E}[\phi_m(Y_i)\phi_n(Y_i)] = \int \phi_m(y)\phi_n(y) dF_{Y_i}(y) = \gamma_m \delta_{mn}, \ 0 \le m, n \le N, \tag{2.1}$$

where

$$\gamma_m = \mathbb{E}\left[{\phi_m}^2(Y_i)\right] = \int {\phi_m}^2(y) dF_{Y_i}(y) \tag{2.2}$$

is a normalized factors and δ_{mn} is Kronecker delta function. The type of orthogonal polynomial is determined by the type of random variable distribution such that the orthogonality will hold with respect to the associated weight function. Then, let $\boldsymbol{i} = (i_1, \cdots, i_d)$ be a multi-index with $|\boldsymbol{i}| = i_1 + \cdots + i_d$. The d-variate Nth-degree gPC basis functions are defined as

$$\Phi_{\boldsymbol{i}}(Y) = \phi_{i_1}(Y_1) \cdots \phi_{i_d}(Y_d), \quad 0 \le |\boldsymbol{i}| \le N . \tag{2.3}$$

which are the basis functions of multivariate polynomial space

$$\mathbb{P}_N^d \equiv \left\{p: \Gamma_Y \to \mathbb{R} \mid p(Y) = \sum_{|\boldsymbol{i}|\leq N} c_i \Phi_{\boldsymbol{i}}(Y)\right\}. \tag{2.4}$$

It follows directly from (2.1) and (2.3) that,

$$\mathbb{E}\left[\Phi_{\boldsymbol{i}}(Y)\Phi_{\boldsymbol{j}}(Y)\right] = \int \Phi_{\boldsymbol{i}}(y)\Phi_{\boldsymbol{j}}(y)dF_Y(y) = \gamma_{\boldsymbol{i}}\delta_{\boldsymbol{ij}} \quad , 0 \leq m, n \leq N \tag{2.5}$$

where $\gamma_{\boldsymbol{i}}$ is a multiplication of one-dimensional normalized factors and $\delta_{\boldsymbol{ij}}$ is *d*-variate Kronecker delta function.

To address the approximation property, define the weighted L^2 space:

$$L^2_{dF_Y}(\Gamma_Y) \equiv \left\{f: \Gamma_Y \to \mathbb{R} \mid \mathbb{E}[f^2(Y)] = \int_{\Gamma_Y} f^2(y)dF_Y(y) < \infty\right\}, \tag{2.6}$$

the inner product

$$< w, v >_{L^2_{dF_Y}} = \int_{\Gamma_Y} w(y)v(y)dF_Y(y), \tag{2.7}$$

and the norm

$$\|w\|_{L^2_{dF_Y}} = \left(\int_{\Gamma_Y} w^2(y)dF_Y(y)\right)^{\frac{1}{2}}. \tag{2.8}$$

Based on the gPC basis functions in polynomial space $\mathbb{P}_N^d$ and the weighted L^2 space defined above, from classical approximation theory, the following conclusion holds:

For any $f \in L^2_{dF_Y}(\Gamma_Y)$, define Nth-degree gPC orthogonal projection as

$$P_N f = \sum_{|\boldsymbol{i}|\leq N} \hat{f}_{\boldsymbol{i}}\, \Phi_{\boldsymbol{i}}(Y) \tag{2.9}$$

$$\hat{f}_{\boldsymbol{i}} = \frac{1}{\gamma_{\boldsymbol{i}}} \int f(y)\, \Phi_{\boldsymbol{i}}(y)\, dF_Y(y), \quad \gamma_{\boldsymbol{i}} = \gamma_{i_1} \cdots \gamma_{i_d}\ . \tag{2.10}$$

Then

$$\|f - P_N f\|_{L^2_{dF_Y}} \to 0, \quad N \to \infty\ . \tag{2.11}$$

That is to say, the function of random variables can be approximated in the form of orthogonal polynomial expansion. The convergence rate depends on the regularity of *f* and the type of orthogonal polynomials $\Phi_{\boldsymbol{i}}(Y)$. This kind of convergence is referred to as *spectral convergence* and we refer this expansion error due to the truncated degree of polynomial space as *gPC projection error*. More details of this section could be found in [25].

2.2 Collocation method on sparse grid

The continuous and discrete random variables share the similar concepts and definitions in Section 2.1, while for the discrete case, the orthogonality is represented by summation instead of integral. From here on, consider the continuous random vector $p = (p_1, \cdots, p_d)$ with density function $\rho(p) = \prod_{i=1}^{d} \rho_i(p_i)$. Note that the normalized factors in (2.2) can be reduced to 1 by normalizing the polynomials in the integration. Thus, the coefficients $\hat{f}$ in (2.10) can be written as

$$\hat{f}_{\boldsymbol{i}} = \int f(p)\, \Phi_{\boldsymbol{i}}(p)\, \rho(p) dp\ . \tag{2.12}$$

The numerical integration rules can provide the approximation to (2.12) using pre-selected points $p^j = (p_1^j, \cdots, p_d^j)$ and the associated weights α^j, $j = 1, \cdots, Q$, such that

$$\tilde{f}_{\boldsymbol{i}} = \sum_{j=1}^{Q} f(p^j)\alpha^j \rightarrow\ \hat{f}_{\boldsymbol{i}},\ Q \rightarrow \infty\ . \tag{2.13}$$

Define

$$I_N f = \sum_{|\boldsymbol{i}| \le N} \tilde{f}_{\boldsymbol{i}}\, \Phi_{\boldsymbol{i}}(Y). \tag{2.14}$$

The difference between $P_N f$ and $I_N f$ is resulted from the numerical integration in coefficient calculation (2.13), and the consequent error $\|P_N f - I_N f\|_{L^2_{dF_Y}}$ is called *aliasing error*.

An important work in collocation method is the selection of nodal set. In one-dimensional case, this problem is readily solved using available numerical integration rules, such as Gaussian quadrature rule and Clenshaw-Curtis rule. The natural generalization to multi-dimensional case is to use tensor products. However, the number of points in tensor product will grow rapidly as the dimension increases, which is known as "curse of dimensionality". When high dimensional uncertainties are considered simultaneously in stochastic processes, the computational burden will be very heavy using tensor products collocation.

Sparse grid collocation provides a useful tool to solve the stochastic problem in high dimensional random space. Smolyak algorithm [26] can construct the nodal set for high dimensional integration which consists of an algebraic sum of low-order tensor products based on one-dimensional quadrature rule in such a way that an integration property for one dimension

is preserved for high dimensions as much as possible [25]. Such construction will result in a great reduction of nodes for integration compared to tensor products.

Define the integration operator $\mathcal{L}_i[f]$ in the i-th dimension

$$\mathcal{L}_i[f] \equiv \sum_{j=1}^{Q} f(p_i^j)\, \alpha_i^j, \tag{2.15}$$

then the Smolyak algorithm gives the following multi-dimensional operator

$$\mathcal{L}[f] = \sum_{K-d \le |\boldsymbol{i}| \le K-1} (-1)^{K-d-|\boldsymbol{i}|} \cdot \binom{d-1}{d-K+|\boldsymbol{i}|} \cdot \left(\mathcal{L}_{i_1} \otimes \cdots \otimes \mathcal{L}_{i_d}\right). \tag{2.16}$$

This operator can calculate the numerical integration (2.9) while preserving the one dimensional integration exactness as much as possible with much fewer nodes than tensor products.

3. Integrated prognostics method for gears

This section provides a brief review on the integrated prognostics method proposed in [6] for cracked gear life prediction. Fig. 2 shows the framework of the approach, which "integrates" model-based part in the left of the dash line and data-driven part in the right. Because the crack occurrence will have impact on the stiffness of the gear, further on the dynamic load on the gear, the dynamic model is necessary to determine the actual dynamic load on gear tooth at different crack lengths. The stiffness of a cracked tooth was calculated using a potential energy method. It is important to account for the load change due to crack since the loading condition determines the stress intensity factor to a large degree, which is the main stress factor appearing in the degradation model, described by Paris' law. The gear finite element model takes the calculated maximum dynamic load in one loading cycle period as input, and the outputs are the mode I and mode II stress intensity factors (SIFs), denoted by KI and KII respectively, at the gear tooth root. The crack propagates in the direction determined by the ratio of KI and KII. With the current crack length, the failure time and the remaining useful life (RUL) distributions can be predicted by propagating the uncertainties through the degradation model. Refer to [6] for more details on the gear stress analysis using finite element model and the dynamic load determination. The main function of the data-driven part is to estimate the crack length (with uncertainty) based on the condition monitoring data measured by sensors. The current measured crack lengths at

certain inspection times will serve as the observations to update the distributions of uncertainties to achieve more accurate RUL prediction, based on the refined parameter and condition estimations for the specific unit. The Bayesian updating method is used in this work to achieve this purpose.

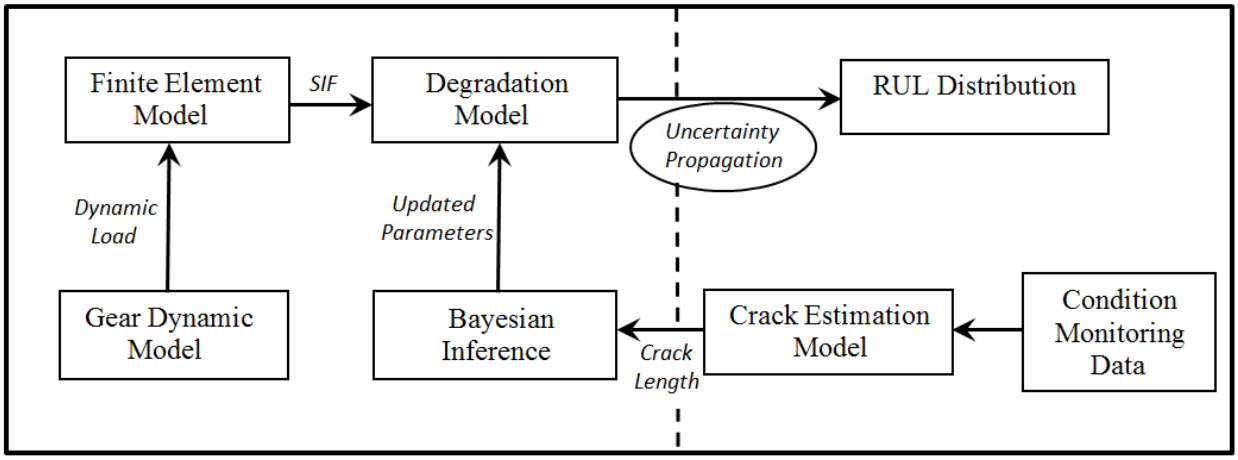

Fig. 2. Framework of the integrated prognostic approach [6]

In the integrated prognostics approach, uncertainties exist in both the model-based part and the data-driven part, which could be the uncertainties in material, loading conditions, measurements inaccuracy, etc. And these uncertainties are propagated to the predicted failure time. To account for the effect of the uncertainties in RUL, which is very meaningful regarding maintenance decision making, an approach is needed to quantify them in a statistical way. In addition, the ways that these uncertainties influence the RUL distribution may be different, and thus it will be helpful to develop an approach to distinguish their roles.

4. The proposed gPC stochastic collocation method for uncertainty quantification in integrated gear prognosis

This section will elaborate the proposed stochastic collocation method for uncertainty quantification and propagation in the above-mentioned integrated gear prognosis framework. First the uncertainty sources involved in this study as well as their roles in the prognosis approach are defined. Then the stochastic collocation method to predict the RUL at a given inspection instant is addressed accounting for these uncertainties based on discretized Paris' law.

Whenever the new observation data is available, it will be taken into Bayesian inference to adjust the statistical properties of those uncertainties so that the distribution of RUL will be updated. Through Bayesian inference, the degree of uncertainty about these random parameters will be reduced, and their statistical properties are supposed to converge to the actual ones. The prediction of RUL is expected to be more accurate after adjusting the parameter distributions each time.

4.1 Modeling of uncertainty sources

In this study, it is assumed that all of the uncertainties considered are categorized into three main sources, which are model inputs uncertainty, measurement uncertainty and model uncertainty.

Paris' law and its evolution forms [27,28,29] are widely used physical models to describe the crack propagation process. When the associated inputs in the model are treated as random variables, the Paris' law becomes a stochastic equation. Denote the set of all these random inputs as $\boldsymbol{\Theta}$, appearing in Paris' model, and divide them into two subsets: updating-uncertainty $\mathbf{U}$, and non-updating-uncertainty $\boldsymbol{R}$. The distributions of uncertainties belonging to $\mathbf{U}$ are unknown, and only the *priors* may be assumed. They will be updated through Bayesian framework using the measured condition data, in order to narrow down the prior distributions and make them converge or approximate to the real distributions. While those uncertainties belonging to $\boldsymbol{R}$ will take well-known distributions, and they are treated as contributors to the likelihood function in the Bayesian method. So this type of uncertainties is named as likelihood-uncertainty in this paper. Both the likelihood-uncertainties and updating-uncertainties contribute to the RUL distribution. Besides likelihood-uncertainty, another contributor to likelihood function is the measurement error.

Measurement error e is defined as the error between the real crack length and the measured length, which is due to sensor precision limits as well as inaccuracy caused by crack estimation methods. It is assumed that the measurement $e = a^{real} - a_{mea}$ follows normal distribution with standard deviation τ,

$$e \sim N(0, \tau^2)$$

Under the assumption that no other uncertainties are involved, it is equivalent to say that the

measured crack length a_{mea} takes normal distribution with the real crack length a^{real} as the mean and the τ as the standard deviation:

$$a_{mea} \sim N(a^{real}, \tau^2) \ . \tag{4.1}$$

A number of existing different physical models to describe the crack propagation process imply that there is no perfect model for all circumstances. The models are selected so as to meet the required accuracy while considering the complexity. In this paper, the simple Paris' law is adopted without considering other possible factors, such as crack closure retard, plasticity, fracture toughness, load ratio etc. The authors in [30] assigned the reason of randomness nature of the crack growth rate to the random unpredictable resistance in material's microstructure. All the above uncertain factors motivate the stochastic modelling of crack propagation. Yang et al. [31] proposed a model by multiplying a stochastic term ε to the deterministic crack growth model (4.2) after investigating the crack propagation in the fastener holes of aircrafts under spectrum loading, and experiments were also conducted to validate this model. The random term ε was assumed to be a lognormally distributed random variable and "accounts for the crack growth rate variability, such as the variabilities due to material cracking resistance, crack geometry, crack modeling, spectrum loading, etc." [32]. This model has the simplest stochastic form and produced conservative reasonable results. So many related work adopted this multiplicative form of model error for crack propagation study in other applications [9,30,32,33,34]. The statistical property of ε could be acquired by least-square fitting of the Paris' law in a log-log scale using the information of crack lengths and associated cycles obtained in the fatigue crack propagation experiments, as reported in [33,35,36]. The experiment data showed the residual ζ in the regression model has Gaussian distribution, and thus, the distribution of ε could be obtained by noticing the relationship of $\varepsilon = \exp(\zeta)$. After this modification, Paris' law can have the following form

$$\frac{da}{dN} = C(\Delta K)^m \, \varepsilon. \tag{4.2}$$

In a word, the uncertainty considered in this paper can be categorized as follows:

$$\begin{cases} \text{measurement error } e \\ \text{model error } \varepsilon \\ \text{Random model inputs} \begin{cases} \text{updating uncertainty } \boldsymbol{U} \\ \text{non} - \text{updating uncertainty } \boldsymbol{R} \end{cases} \end{cases} .$$

As for the problem that among all the random inputs involved in the physical model, which

belong to which subset is a matter to be decided according to the specific application.

4.2 Remaining useful life prediction

The remaining useful life prediction is performed at every inspection point when the current crack length is estimated. At one of such points *t*, suppose the observed current crack length is a_t. The crack will propagate according to the Paris' law until it reaches the critical length a_C, when the gear is considered failed.

By exchanging the position of differentiation, the modified Paris' law considering model error is written in Equation (4.3), where ΔK represents the range of the stress intensity factor, which is an essential factor of the stress field near crack tip and generally obtained by finite element analysis. It could be affected by various factors. However, in this paper, it is considered as a function of crack length and load only which was written as $\Delta K(a)$. When the FE is used to calculate this relationship, the dynamic load is a function of crack length too.

$$\frac{dN}{da} = \frac{1}{C(\Delta K(a))^m \varepsilon} \tag{4.3}$$

Let the current inspection cycle be N_t and the crack increment be Δa. The modified Paris' law is discretized by finite difference method:

$$\Delta N_{i+1} = N_{i+1} - N_i = \Delta a \left[C(\Delta K(a_i))^m \varepsilon\right]^{-1},\ i = t, t+1, \cdots. \tag{4.4}$$

The summation $\sum \Delta N_i, i = t, t+1, \cdots$ from the current crack length at inspection cycle N_t until the critical length a_C is the total remaining useful cycles, which is the RUL we are interested in. The entire failure time could be obtained by $N_t + \sum \Delta N_i, i = t, t+1, \cdots$.

The crack propagation itself is affected by various uncertainties, such as material, lubrication, speed, loading and damage initial conditions. All of the potential factors have the representations in Paris' law or other physical models, which are considered as stochastic differential equations governing the crack propagation process. The RUL distribution is determined by this stochastic process due to various sources of uncertainty. When more uncertainty factors are effectively considered, typically the prediction will be more accurate. gPC stochastic collocation method with Smolyak algorithm is capable of dealing with high dimensional random space with fast convergence rate. So instead of using Monte Carlo simulation to quantify the uncertainty in the predicted RUL, a gPC stochastic collocation method is to be presented here.

We parameterize the probability space by finding the finite set of uncertainty factors in the gear health degradation. The random parameters in this set are denoted by $\boldsymbol{\xi} = (\xi_1, \cdots \xi_d)$, assumed to be independently and identically distributed (iid). The density function can be written as $\rho(\boldsymbol{\xi}) = \prod_{i=1}^{d} \rho_i(\xi_i)$. Corresponding to the type of distribution, $\{\Phi_{\boldsymbol{i}}(\boldsymbol{\xi}) \in \mathbb{P}_N^d,\ 0 \leq |\boldsymbol{i}| \leq N\}$ are the basis orthorgonal polynomials. Denote the failure time by T, which is the quantity of interest. T is a function of these random parameters $\boldsymbol{\xi}$ through the Paris' law,

$$T = S\big(a(\boldsymbol{\xi})\big) = T(\boldsymbol{\xi}). \tag{4.5}$$

T is the loading cycles when the crack length reaches the critical length.

Firstly, nodal set is selected using Smolyak algorithm, which is $\{\xi^j,\ j = 1, \cdots, Q\}$. Based on the proper integration rule, the associated weights $\alpha^j, j = 1, \cdots, Q$, are also available. Secondly, the failure times at these nodes are obtained by propagating the crack through Paris' law in a deterministic way. Denote them as $\tilde{T}^j = T(\xi^j), j = 1, \cdots, Q$. After that, we use the truncated N-th degree of gPC expansion, $T_N = P_N T$, to approximate T,

$$T_N = \sum_{l=1}^{M} \widehat{\omega}_l\, \Phi_l(\boldsymbol{\xi}), \tag{4.6}$$

$$T_N \to T \quad \text{as} \quad M \to \infty. \tag{4.7}$$

From (2.7), we have

$$\widehat{\omega}_l = \int_{\Gamma} T(\boldsymbol{\xi})\, \Phi_l(\boldsymbol{\xi}) \rho(\boldsymbol{\xi})\, \mathrm{d}\boldsymbol{\xi}. \tag{4.8}$$

Based on (2.10), numerical integration could be used to calculate $\widetilde{\omega}_l^N$ to approximate $\widehat{\omega}_l$,

$$\widetilde{\omega}_l^N = \sum_{l=1}^{Q} \tilde{T}^j \cdot \Phi_l\big(\xi^j\big) \cdot \alpha^j, \tag{4.9}$$

$$\widetilde{\omega}_l^N \to \widehat{\omega}_l \quad \text{as} \quad Q \to \infty. \tag{4.10}$$

Finally, we replace $\widehat{\omega}_l$ in (3.3) by $\widetilde{\omega}_l^N$, obtaining

$$I_N T = \bar{T}_N = \sum_{l=1}^{M} \widetilde{\omega}_l^N\, \Phi_l(\boldsymbol{\xi}), \tag{4.11}$$

$$\bar{T}_N \to T_N \quad \text{as} \quad Q \to \infty. \tag{4.12}$$

Through the triangular inequality involving *projection error* and the *aliasing error*, $\bar{T}_N$ will converge to T, which is guaranteed by (4.7) and (4.12). $\bar{T}_N$ can be close enough to T to the required degree as the order of polynomial and the number of nodes for integration increases. If

the error of numerically solving T is also considered, the approximation is still valid as long as such numerical method gives convergent solution to the deterministic problem. The idea of the proof can be found in [10]. The result obtained by the proposed approach is an approximate solution in the form of polynomial expansion with respect to the standard random variables. Comparing to Monte Carlo sampling, two merits of the new approach are distinct. One is the reduction of computing time because the executions of the deterministic problem, say, Paris' law equation here, are needed only at the selected nodes in the sparse grid. The other merit is that the post-processing work is easy to do. As we can see, the failure time is represented as polynomial expansion with standard random variables. Evaluation of polynomials is a trivial work, and thus the density function of the interested random quantity and the associated moments can be obtained in a very efficient fashion.

4.3 Prediction updating using Bayesian method

The appealing feature of integrated prognostics is the ability to incorporate condition monitoring data into prediction. These data carries specific valuable health condition information for a specific gear under specific testing environment. The intelligence brought in by the data creates an opportunity to adjust the physical model parameters for the current gear being monitored, and to make the RUL prediction more accurate and more distinguished from other gears. As we know, for a specific gear, the distributions of some uncertainty factors should be narrow or even a deterministic value, such as the material uncertainty. For the gear population, though, the underlying uncertainty results from manufacturing processes, monitoring process and operating environment. So the distributions of uncertain parameters associated with the gear population should be wider than those for specific gear. With the real condition data specific to the gear under monitoring, we should be able to reduce the uncertainty in these parameters. Bayesian inference is a commonly used tool to assimilate the data to enhance the possibility of existence of truth, and will be used in this work to update the distributions of the uncertainties.

To describe the general application of gPC stochastic collocation method in integrating new observations of current health condition into health prognosis through the Bayesian inference, as mentioned in Section 4.1, we divide the set of all potential random model inputs, $\boldsymbol{\Theta}$, appearing in Paris' model into two subsets: updating-uncertainty $\boldsymbol{U}$, and non-updating-uncertainty (likelihood-uncertainty) $\boldsymbol{R}$. The health condition data in the gear crack propagation is the crack length at inspection time. Denote the random variable of crack length as a, the updating-uncertainty vector

as $\boldsymbol{u}$, and likelihood-uncertainty vector as $\boldsymbol{r}$. The formula of Bayesian rule is:

$$f_{post}(\boldsymbol{u}|a) = \frac{L(a|\boldsymbol{u})f_{prior}(\boldsymbol{u})}{\int L(a|\boldsymbol{u})f_{prior}(\boldsymbol{u})d\boldsymbol{u}}, \tag{4.13}$$

where $L(a|\boldsymbol{u})$ is the likelihood function contributed by the measurement error and likelihood-uncertainties. The purpose of Bayesian inference here is to update the distributions of uncertainties in $\boldsymbol{U}$ based on the crack measurements.

Given a fixed value of $\boldsymbol{u}$, the likelihood to observe a crack length at a given inspection cycles depends on two factors: model error ε, measurement error e and likelihood-uncertainty $\boldsymbol{r}$.

Assume that the increment number of cycles is ΔN and the inspection time interval is $\lambda\Delta N$. In such a period, the crack propagates following the discretized Paris' law in (4.14),

$$\begin{cases} a_{i+1} = a\big((i+1)\Delta N\big) = a(i\Delta N) + (\Delta N)C\big[\Delta K\big(a(i\Delta N)\big)\big]^m\varepsilon, \;\; i = 0,1,\cdots,\lambda-1 \\ a(0) = a_{curr\_cycle} \end{cases} \tag{4.14}$$

At the end of the period, $a_{j\lambda}, j = 1,2,\cdots$, obtained by (4.14) is a random variable due to the influence of randomness in likelihood-uncertainties $\boldsymbol{r}$ as well as the model error ε. For example, beginning with the "current cycle", the crack length at next inspection time $t = \lambda\Delta N$, i.e., when j=1, is predicted by (4.14) to be $a_{next\_cycle} = a_\lambda = a(\lambda\Delta N)$. Here, since the randomness of model error ε is embodied in every small discrete step in (4.14), the total accumulated effect of ε on the crack length estimation at certain inspection time, relatively long compared to cycles increment, mainly relies on its mean because of central limit theory. Hence, without much loss of accuracy, we assume that the distribution of $a_{j\lambda}$ is only affected by likelihood-uncertainties even though the realization of ε in each propagation step in (4.14) is sampled from its known distribution. Let the density function of $a_{j\lambda}$ be $h_j(a)$, which also can be regarded as the crack distribution at inspection time $j\lambda\Delta N$ due to non-updating-uncertainties $\boldsymbol{R}$ in the model inputs. To avoid confusion, we use a new random variable a_j^R instead of $a_{j\lambda}$ to represent the crack length at inspection time $j\lambda\Delta N$ due to non-updating-uncertainties $\mathcal{R}$.

Furthermore, considering the measurement error, the observed crack length at such inspection cycle $j\lambda\Delta N$ should have the following normal distribution:

$$a_j^{obs} \sim N\big(a_j^R, \tau^2\big), \;\; j = 1,2,\cdots. \tag{4.15}$$

Let the density function of the observed crack length due to measurement error, i.e., $N(a_j^R, \tau^2)$, be $g_j(a)$. Then the likelihood to observe the crack length $a_j^{obs} = a_{j\_0}^{obs}$ at inspection time j can be

formulated as

$$L\left(a_j^{obs} = a_{j\_0}^{obs} \middle| \boldsymbol{u}\right) = \int g_j\left(a \middle| a_j^R = a_{j\_0}^{obs}\right) h_j(a)\, \mathrm{d}a. \tag{4.16}$$

This formulation of the likelihood function accounts for the effects of both non-updating-uncertainties and the measurement error on the observations. In the likelihood function, $g_j(a|a_j^R = a_{j\_0}^{obs})$ is known. However $h_j(a)$ is unknown, and can only be obtained through uncertainty propagation. If we have high dimensional uncertainties in the set of $\boldsymbol{R}$, getting $h_j(a)$ is a time-consuming task using Monte Carlo simulation. Thus, to improve the computation efficiency, we employ gPC stochastic collocation method to replace Monte Carlo simulation to perform this task. Suppose the likelihood uncertainties in $\boldsymbol{R}$ to be iid random variables $\boldsymbol{r} = (r_1, \cdots, r_D)$. The crack length a_j^R at inspection time j is a random variable due to $\boldsymbol{r}$. It can be approximated by orthogonal polynomial expansion in $\mathbb{P}_N^d$,

$$a_j^R = \sum_{\boldsymbol{i} \le N} \tilde{\mu}_{\mathbf{ij}} \Phi_{\boldsymbol{i}}(\boldsymbol{r}), \qquad j = 1,2,\cdots \tag{4.17}$$

$$\tilde{\mu}_{\mathbf{ij}} = \sum_{l=1}^{Q} a_j^R(\boldsymbol{r}^l)\Phi_{\boldsymbol{i}}(\boldsymbol{r})\alpha^l, \qquad l = 1,2,\cdots,Q \tag{4.18}$$

where $\boldsymbol{r}^l$ is the pre-selected nodes and α^l are the associated weights for integration.

As discussed above, the likelihood function can be computed. Using Bayesian inference as shown in (4.13), the distributions of uncertainty factors in the set of $\boldsymbol{U}$ will be updated. With the updated distributions of parameters, the RUL from that inspection time can be calculated using gPC stochastic collocation method described in Section 4.2.

The last problem needs to be addressed is how to determine the prior distributions of the updating uncertainties. First assuming that several historical paths of degradation data are available, which imply the population statistic characteristics, these real paths will be fitted to find the optimal values of the updating parameters in $\boldsymbol{U}$ in a sense of least-square. The existing historical set containing N degradation histories is denoted by $\mathcal{P}$. Each path $\mathcal{P}_i$ composes of M inspection time instances $t_i^j, j = 1, \cdots, M$ and the associated crack length $a_i^{j\_obs}$ estimated at such inspections.

$$\mathcal{P} = \{\mathcal{P}_i|, i = 1, \cdots, N\} \tag{4.19}$$

$$\mathcal{P}_i = (t_i^j, a_i^{j\_obs}),\ j = 1, \cdots, M \tag{4.20}$$

Next, applying Paris' law to generate degradation paths $\mathcal{P}_i'$ with updating parameters $\boldsymbol{u}$, obtaining the approximate crack length $a_i^{j\_app}(\boldsymbol{u})$ at the inspection time $t_i^j, j = 1, \cdots, M$.

$$\mathcal{P}_i' = (t_i^j,\, a_i^{j\_app}(\boldsymbol{u})),\ j = 1, \cdots,\, M \tag{4.21}$$

Define $e_i^j(\boldsymbol{u}) = a_i^{j\_obs} - a_i^{j\_app}(\boldsymbol{u})$, then the optimal $\boldsymbol{u}_{op}^i$ is found to be such that

$$\sum_{j=1}^{M}(e_i^j(\boldsymbol{u}_{op}^i))^2 \leq \sum_{j=1}^{M}(e_i^j(\boldsymbol{u}))^2\,,\ \forall \boldsymbol{u} \tag{4.22}$$

Lastly, prior distribution of $\boldsymbol{u}$ will be determined by fitting these $\boldsymbol{u}_{op}^i,\ i = 1, \cdots, N$.

5. Example

In this section, we present a numerical example on integrated gear prognosis using the proposed gPC stochastic collocation approach. The uncertainties considered include model error ε, measurement error e, and the two material random parameters in Paris' law, C and m. Other parameters appearing in the Paris' law are treated as deterministic. Divide the random inputs appearing in Paris' law into two subsets: $\boldsymbol{R} = \{C\}, \boldsymbol{U} = \{m\}$. The simulated crack propagation data, i.e., the degradation paths, serves as the observations during the operation of real gear system. In RUL prediction, $\boldsymbol{\xi} = (C, m)$ is taken to be the cause of life variation. All the uncertainties, including model error, measurement error as well as the two material random parameters, are considered in the degradation path generation. These degradation paths are partitioned into training set and test set. The training process is for obtaining prior for the updating uncertainty, while the testing process is for validating the proposed method.

5.1 Introduction

The FE model for gear with a crack at the root is built using software FRANC2D. Because of the geometrical symmetry of spur gear and the uniform loading distribution on the tooth width, two-dimensional FE model, consuming less computational work compared to 3D model, is able to meet the accuracy requirements. The gearbox parameters are the same as those we used in [6], so that we can compare the method proposed in this paper. And for easier access to those information in this paper, we present them again: Table 1 lists the material and geometry properties of this specific spur gear and the FE model with curved crack propagation path is shown in Fig. 3.

Table 1. Material properties and main geometry parameters [6].

Young's modulus (Pa)	Poisson's ratio	Module (mm)	Diametral pitch (in^{-1})	Base circle radius (mm)	Outer circle (mm)	Pressure angle (deg)	Teeth No.
2.068e11	0.3	3.2	8	28.34	33.3	20	19

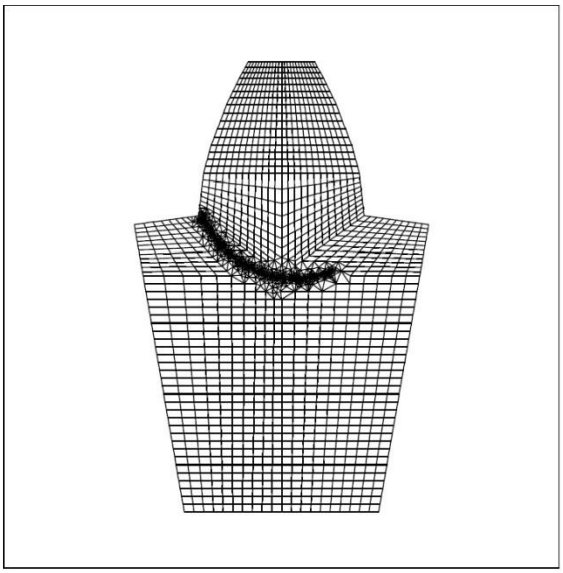

Fig. 3. 2D FE model for spur gear tooth [6]

The dynamic load on the contact points when the pair of teeth meshing with each other is calculated by a 6-DOF dynamic model. During a meshing period, it is the maximum dynamic load on the cracked tooth that is selected to apply on the associated contact point, which in this example, appears at the rotation angle of 13.89 degree. Through the FE analysis with the dynamic load calculated at different crack length, the history of stress intensity factor as a function of crack length is shown in Fig.4. Additionally, Fig. 4 includes the history of maximum dynamic load at each crack length. Polynomial curve fitting gives a continuous form to the SIF, which facilitates in solving the Paris' equation numerically.

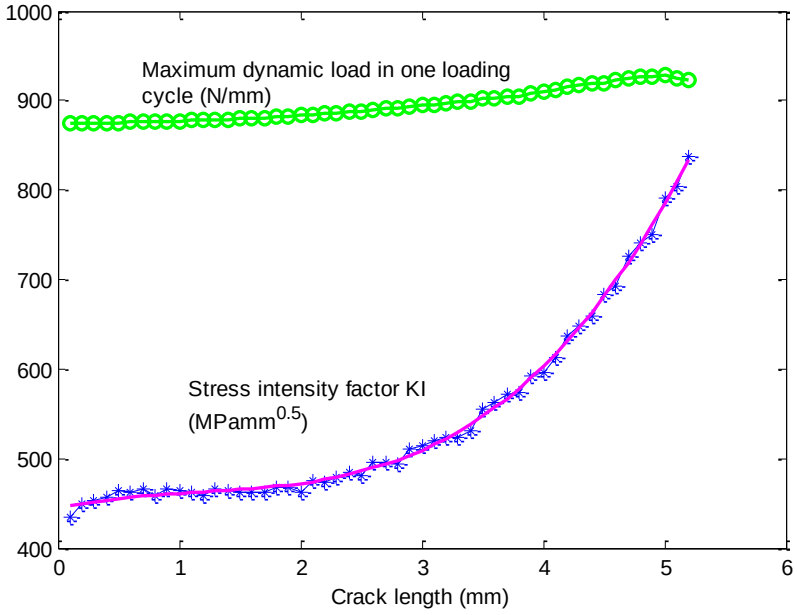

Fig. 4. Stress intensity factor at different crack lengths [6]

When generating the degradation paths, material parameters C and m are sampled from the prescribed normal distributions, respectively. However, the model error ε is sampled from its assumed distribution in each propagation step. At every inspection time, crack length is simulated by Equation (4.14) and estimated by adding a random deviation sample of the measurement error e to the simulated length. All these paths and the values of parameter m in these paths are recorded. These values of m are considered as the real values to generate specific degradation paths.

To generate the simulated degradation paths, the following values and distributions for the parameters involved are assumed: $m \sim N(1.4354, 0.2^2)$, $C \sim N(9.12e-11, (1e-12)^2)$, $\tau = 0.15$, $\varepsilon \sim Ln\,(0.8924, 0.2128)^2$.

It is worth noting that here the uncertainty regarding m is the distribution for the gear population, not for the specific gear being monitored. In this example, 10 degradation paths are generated according to Equation (4.14) until the critical crack length a_c, as shown in Fig. 5. Seven of them in blue consist of the training set, and the three remaining in bold magenta are for testing. The selection of the two groups is random in theory while there is a underlying preference in this paper. That is, the paths bearing "*m*" which are far from the mean of prior have

priority to be selected in order to better show the capability of tuning parameters. In Fig. 5, the paths with the longest (path #1) and shortest (path #4) failure times are selected in test set. Besides, path #7 which has similar value of "*m*" as that in prior is also targeted to illustrate the stability of proposed method in an opposite perspective.

Apart from validating the effectiveness of the proposed gPC collocation based prognostics method, which aims to produce correct RUL prediction using gPC technique, the computational efficiency of this proposed method is also demonstrated by comparing with Monte Carlo simulation. The results are shown in the next two subsections.

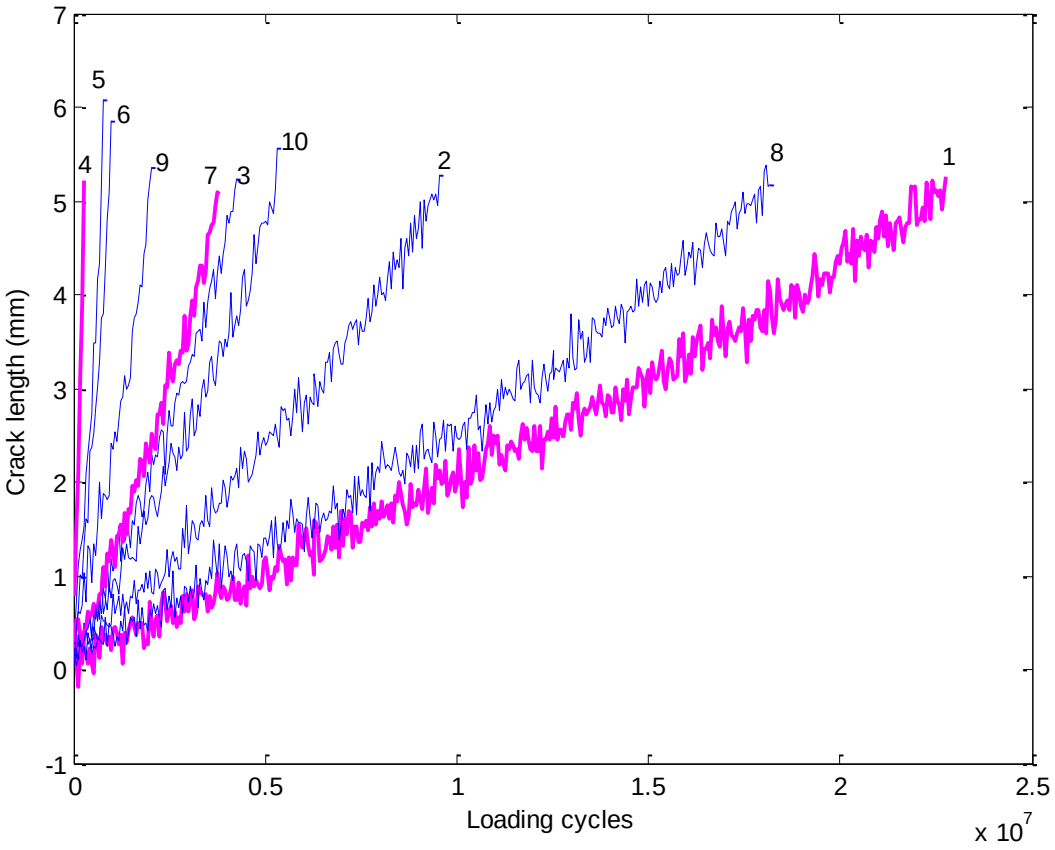

Fig. 5. Ten degradation paths generated using prescribed parameters

5.2 Results

The 10 generated degradation paths with parameters assumed in Section 5.1 are summarized in Table 2. The failure times, real values of "*m*" generating the associated paths as well as the trained ones are shown in this table. The testing set consist of paths #1, #4 and #7. Normal

distribution is used to fit the other 7 paths to obtain the prior distribution of m:

$$m \sim N(1.4029, 0.1878^2)$$

Table 2. The real values and the trained values of m

Path #	Failure cycles	Real value	Trained value
1	**22.75e6**	**1.1009**	**-**
2	9.55e6	1.2403	1.2365
3	4.25e6	1.3724	1.3671
4	**0.3e6**	**1.7968**	**-**
5	0.8e6	1.6454	1.646
6	1.0e6	1.6098	1.6064
7	**3.8e6**	**1.3884**	**-**
8	18.15e6	1.1388	1.1377
9	2.05e6	1.4863	1.4893
10	5.3e6	1.3364	1.3375

At each updating time, the posterior distribution of m will become the prior distribution for the next updating time.

The only likelihood-uncertainty in this example is the material parameter C following normal distribution. Corresponding to the type of distribution, the up to third-order Hermite orthogonal polynomials are used. To calculate the $h_j(a)$ at inspection time j in the likelihood function in Bayesian inference defined in Section 4.3, a sparse nodal set containing 7 points is selected.

The updating-uncertainty here is the material parameter m, which also follows normal distribution. At each inspection time, this distribution is updated by Bayesian inference. From that inspection time, the RUL is calculated based on the distributions of both C and m. To achieve this, a two-dimensional sparse grid with 13 nodes is selected, following the procedure described in Section 4.2. The third-order polynomial space is selected to achieve the RUL distribution calculation.

Table 3, 4 and 5 show the updating results for both m and the failure time. From these results, the convergence trend to their actual values is obvious. The RUL adjustment depends on the

adjustment of m. Starting with its prior value 1.4037, m approaches its real values gradually, as the condition monitoring data on the crack length are fused into prediction by Bayesian inference. Meanwhile, the uncertainty reduction in both m and failure time is apparent. The failure time distributions for path #1, #4 and #7 are shown in Fig. 6, 7 and 8, respectively, from which we can observe that with the updating of the m distribution at certain inspection cycles, the predicted failure time distribution becomes narrower and its mean is approaching the real failure time. The prediction results agree very well with those reported in [6], which used simulation in uncertainty quantification. This example only utilizes low degree of polynomial as well as few collocation nodes to achieve acceptable accuracy. In the following section, comparative study is conducted to illustrate the effect of truncated polynomial degree and number of collocation nodes on the accuracy of gPC. With the increase both of the two factors, the gPC accuracy can be improved.

Table 3. Testing results for path #1 (real m=1.1009, real failure time=2.275e7 cycles)

Inspection cycle	Crack length (mm)	Mean of m	Std of m	Mean of Failure time	Std of Failure time
0	0.1	1.4029	0.1878	6.9703e6	9.2389e6
0.7e7	1.6849	1.1257	0.0153	1.947e7	1.2064e6
1.4e7	2.9092	1.1024	0.0099	2.2493e7	5.5313e5
2.1e7	4.6018	1.0991	0.0073	2.2789e7	9.3263e4

Table 4. Testing results for path #4 (real m=1.7968, real failure time =0.3e6 cycles)

Inspection cycle	Crack length (mm)	Mean of m	Std of m	Mean of Failure time	Std of Failure time
0	0.1	1.4029	0.1878	6.7118e6	8.8709e6
0.1e6	1.4971	1.7924	0.0184	3.0302e5	2.3163e4
0.2e6	3.1079	1.8008	0.0114	2.8527e5	7.4258e3

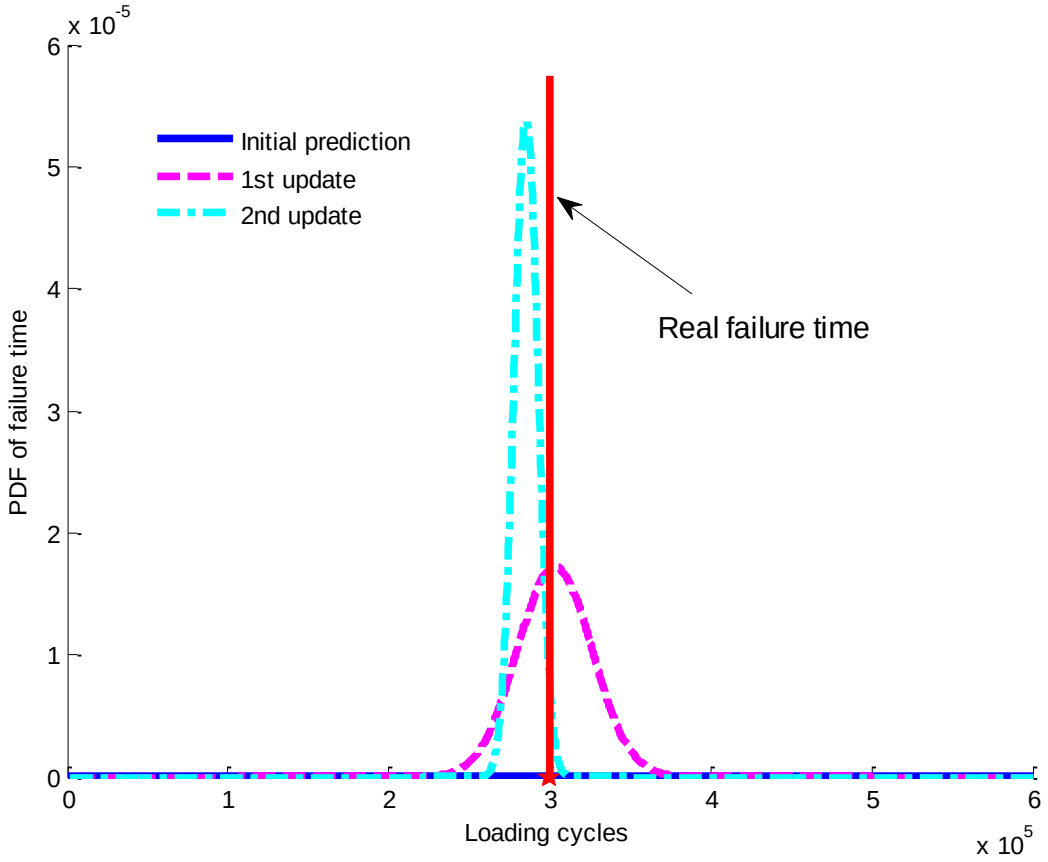

Fig. 7. Failure time distribution prediction with updates for path #4

Table 5. Testing results for path #7 (real m=1.3884, real failure time=3.8e6 cycles)

Cycles when updating m	Crack length (mm)	Mean of m	Std of m	Mean of Failure time	Std of Failure time
0	0.1	1.4029	0.1878	6.7092e6	8.8759e6
1.2e6	1.4387	1.3839	0.0185	3.8888e6	3.1581e5
2.4e6	3.022	1.3947	0.0119	3.6268e6	9.7808e4
3.6e6	4.7519	1.3799	0.007	3.8027e6	1.0637e4

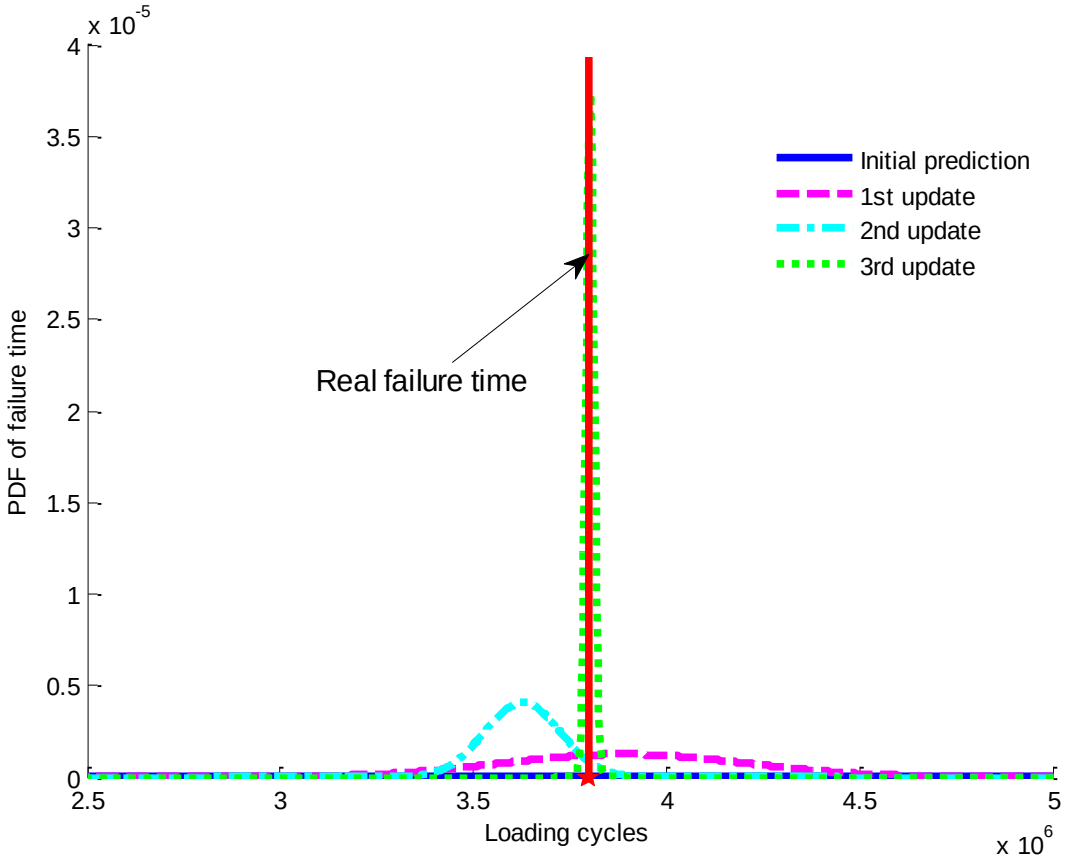

Fig. 8. Failure time distribution prediction with updates for path #7

5.3 Comparative study

The accuracy of gPC is controlled by the error of projection in (4.6) and the error of numerical integration in (4.9). To be more specific, the two controllable factors, truncated polynomial degree and number of collocation nodes in the selected numerical integration rule, determine the accuracy of gPC collocation method. A comparative study is conducted in this section to illustrate the effects of the two factors. In this investigation, we select the remaining useful life (RUL) prediction as the representative case, since it involves two uncertainty factors, both C and m. And we focus on the entire failure time covering from the initial crack length to the critical length, given the known distribution of parameters as random inputs.

In this investigation, due to the lack of explicit form of exact solution, we consider the result obtained using Monte-Carlo simulation as the real distribution of the failure time, so as to compare with the results obtained via PCE with different degrees and nodes. Comparative

studies are conducted to demonstrate 1) the effects caused by truncated polynomial degree by fixing the number of integration nodes, and 2) the effects caused by number of integration rules by fixing the truncated polynomial degree. The mean and standard deviation of RUL predicted by gPC are compared with those obtained by Monte Carlo simulation, which are considered as the real distribution. The results are tabulated in Table 6 and Table 7, respectively. As the number of integration nodes increase, with a fixed sufficient truncated degree, the mean and standard deviation produced by gPC approach the real ones, as shown in Table 6. On the other hand, the accuracy improvement by increasing the truncated polynomial degree with fixed number of integration nodes can also be seen, as shown in Table 7. It is worth noting that the latter type of improvement is limited by the integration nodes. It is possible that the higher order polynomial may not perform better than the lower order one, unless we increase the integration accuracy at the same time, i.e., the number of integration nodes. It is concluded that gPC accuracy can be improved by increasing both the truncated polynomial degree and number of integration nodes. But it should be noted that the increase in polynomial degree and integration nodes will lead to the increase in computation burden.

Table 6. Effect of increasing number of integration nodes with 6^{th} order polynomial space

RUL	5 ndoes	13 nodes	29 nodes	53 nodes	89 nodes	137 nodes	5000 MC
Mean	5.3733e6	5.9348e6	6.038e6	6.1427e6	6.1837e6	6.1943e6	6.1974e6
Std	9.5945e9	1.1115e7	1.214e7	1.28e7	1.3591e7	1.3867e7	1.3912e7

Table 7. Effect of increasing truncated polynomial degree with 137 integration nodes

RUL	2^{st} order	3^{nd} order	4^{rd} order	6^{th} order	7^{th} order	8^{th} order	5000 MC
Mean	6.0472e6	6.087e6	6.161e6	6.1943e6	6.1914e6	6.2072e6	6.1974e6
Std	1.0315e7	1.1954e7	1.3042e7	1.3867e7	1.3922e7	1.413e7	1.3912e7

5.4 Efficiency investigation for the proposed approach

The implementation of the proposed gPC collocation based prognostics method is conducted in MATLAB. The code includes two phases: Bayesian update and RUL prediction. In this subsection, the comparison of computational time consumed by gPC collocation and Monte Carlo simulation will be investigated. Path #1 is selected as an example.

Monte Carlo simulation is a random sampling method. Actually, the nature of gPC collocation

is also simply a process of sampling. However, it samples following "rules" which decide the selection of integration points. Because of the representation as a form of polynomial expansion, the time needed for the evaluation of a polynomial is negligible compared to the execution of the model deterministically. Hence, the computational cost saved by gPC collocation method mainly comes from the reduction of times to run the model.

To explain it more specifically, take the RUL calculation as instance. To calculate RUL from certain inspection time, let's assume it will take around 2 seconds to compute the failure time using discrete Paris' law. If Monte Carlo simulation is used as in [6], at least 1000 iterations is required to get a good picture of failure time statistics, which will take around 90 minutes. In contrast, gPC stochastic collocation only needs 13 nodes to give agreed results, which means the Paris' equation only needs to be solved deterministically at these 13 predetermined points. So the time consumed by gPC is only around 26 seconds. That is, the proposed integrated prognosis approach is thousands of times faster comparing to that using the simulation method.

To compare the results obtained by Monte Carlo simulation and gPC collocation method, the error between the predicted failure time and the real failure time defined in (5.1) is used to measure the prediction performance of these two approaches. Denote $\rho(t)$ as the PDF of failure time predicted at the last inspection cycle. The real failure time known for validation is t_r. The prediction error is defined as a weighted L^2-norm,

$$\left(\int (t - t_r)^2 \rho(t) \mathrm{dt}\right)^{\frac{1}{2}}. \tag{5.1}$$

Table 6 shows the comparison of the prediction errors as well as the computational time of Monte Carlo simulation and gPC collocation method. From this table, it is seen that gPC not only produces satisfactory results but also saves much computation efforts. Furthermore, the significant computation efficiency improvement provided by the gPC technique enables us to consider the randomness of material parameter C which contributes to the likelihood function in Bayesian inference, while in the previous work [6], C is only treated as a constant value due to heavy computation burden.

6. Conclusions

In this paper, based on an integrated prognostics framework for gear remaining life

prediction, a stochastic collocation approach is developed for efficient integrated gear health prognosis. Instead of using simulation, stochastic collocation methods based on generalized polynomial chaos expansion are utilized to evaluate gear remaining useful life prediction uncertainty as well as the likelihood function in Bayesian inference. Two categories of random parameters appearing in Paris' law are also defined.

The results in the numerical example demonstrate that the proposed gPC stochastic collocation approach for integrated gear prognosis can effectively and efficiently adjust the model parameters based on the observed degradation data, and thus lead to more accurate remaining useful life prediction. The significant computation efficiency improvement provided by this approach enable us to consider more uncertain factors in a practical way. The proposed approach can be potentially applied to other application involving crack and other damage propagations. The proposed integrated prognostics approach can greatly improve the efficiency by utilizing the gPC method. This approach has the potential to be applied to other rotating components, such as bearings, shafts, and more complex gearbox systems. It also has the potential to be applied to structures such as aircraft structures, bridges, pipelines, pressure vessels, etc. These potential applications require investigations in building the physical models for these components and structures, integration of the gPC methods, updating methodologies, etc. The proposed method can only be used after crack initiation. Diagnostics methods are needed to detect the crack initiation, and after that, the prognostics methods, such as the one we propose in this paper, can be used to predict the failure times.

Acknowledgments

This research is supported by Le Fonds québécois de la recherche sur la nature et les technologies (FQRNT) and the Natural Sciences and Engineering Research Council of Canada (NSERC)

Table 6. Comparison of Monte Carlo simulation and gPC collocation method

Approach	Time in two phases		Total time	RUL prediction error (cycle)
	Bayesian update	RUL prediction	Integrated method	
Monte Carlo simulation	1000 loops	1000 loops	-	9.9325e4
1st update	146830 sec	5066.5 sec	≈42 hours and 12 min	
2nd update	151540 sec	3439.5 sec	≈43 hours and 30 min	
3rd update	147470 sec	725.5 sec	≈41 hours and 10 min	
gPC collocation method	7 points	13 points	-	9.8624e4
1st update	959.7 sec	65.1 sec	≈17.1 min	
2nd update	1016.7 sec	44.2 sec	≈17.7 min	
3rd update	963.5 sec	9.6 sec	≈16.2 min	

References

[1] A. K. S. Jardine, D. M. Lin, D. Banjevic, A review on machinery diagnostics and prognostics implementing condition-based maintenance, Mech. Syst. Signal Pr. 20 (2006) 1483-1510.

[2] M. Dong, D. He, A segmental hidden semi-Markov model (HSMM)-based diagnostics and prognostics framework and methodology, Mech. Syst. Signal Pr. 21 (2007) 2248-2266.

[3] Z. Tian, M. J. Zuo, S. Wu, Crack propagation assessment for spur gears using model-based analysis and simulation, J. Intell. Manuf. 23 (2012) 239-253.

[4] C. J. Li, H. Lee, Gear fatigue crack prognosis using embedded model, gear dynamic model and fracture mechanics, Mech. Syst. Signal Pr. 19 (2005) 836–846.

[5] S. Marble, B. P. Morton, Predicting the remaining life of propulsion system bearings, In Proceedings of the 2006 IEEE Aerospace Conference, Big Sky, MT, USA.

[6] F. Zhao, Z. Tian, Y. Zeng, Uncertainty quantification in gear remaining useful life prediction through an integrated prognostics method, IEEE T. Reliab. Accepted. (May be accessed at: http://users.encs.concordia.ca/~tian/index_files/Papers/IEEE_TR_Zhao_2012.pdf)

[7] G. J. Kacprzynski, A. Sarlashkar, M. J. Roemer, A. Hess, G. Hardman, Predicting remaining life by fusing the physics of failure modeling with diagnostics, JOM. 56 (2004) 29-35.

[8] A. Coppe, R. T. Haftka, N. H. Kim, Uncertainty reduction of damage growth properties using structural health monitoring, J. Aircraft, 47 (2010) 2030-2038.

[9] S. Sankararaman, Y. Ling, S. Mahadevan, Uncertainty quantification and model validation for fatigue crack growth prediction, Eng. Fract. Mech. 78 (2011) 1487-1504.

[10] D. Xiu**,** Efficient collocational approach for parametric uncertainty analysis, Comm. Comput. Phys. 2(2007) 293-309.

[11] D. Xiu and G. E. Karniadakis, The Wiener-Askey polynomial chaos for stochastic differential equations, Siam J. Sci. Comput. 24 (2002), 619-644.

[12] P. Pettersson, G. Iaccarino, J. Nordström, Numerical analysis of the Burgers' equation in the presence of uncertainty, J. Comput. Phys. (2009), doi:10.1016/j.jcp.2009.08.012

[13] T. Chantrasmi, P. Constantine, N. Etemadiz, G. Iaccarino, Q. Wang, Uncertainty quantification in simple linear and non-linear problems, Annual Research Briefs (2006).

[14] T. Chantrasmi, A. Doostan, G. Iaccarino, Padé–Legendre, Approximants for uncertainty analysis with discontinuous response surfaces, J. Comput. Phys. 228 (2009) 7159–7180.

[15] H. N. Najm, B. J. Debusschere, Y. M. Marzouk, S. Widmer, O. P. Le Maître, Uncertainty quantification in chemical systems, Int. J. Numer. Meth. Eng. 80 (2009) 789-814.

[16] M. S. Eldred, Recent Advances in Non-intrusive polynomial chaos and stochastic collocation methods for uncertainty analysis and design, in Proceedings of the 11th AIAA Nondeterministic Approaches Conference, No. AIAA-2009-2274, Palm Springs, CA, 2009.

[17] D. Ghosh and C. Farhat, Strain and stress computations in stochastic finite element methods, Internat. J. Numer. Methods Engrg. 2007

[18] B. J. Debusschere, H. N. Najm, P. P. Lébay, O. M. Knio, R. G. Ghanem, O. P. Le Maître, Numerical challenges in the use of polynomial chaos representations for stochastic process, Siam J. Sci. Comput. 26 (2004) pp. 698-719.

[19] M. S. Eldred, C. G. Webster, P. Constantine, Evaluation of non-intrusive approaches for Wiener-Askey generalized polynomial chaos, in the Proceedings of the 10th AIAA Nondeterministic Approaches Conference, No. AIAA-2008-1892, Schaumburg, IL, 2008

[20] M. T. Reagan, H. N. Najm, B. J. Debusschere, O. P. Le Maître, O.M. Knio, R. G. Ghanem, Spectral stochastic uncertainty quantification in chemical systems, Combust. Theor. Model. 8 (2004) 607-632.

[21] C. Canuto, M. Y. Hussaini, A. Quarteroni, T. A. Zang, Spectral Methods in Fluid Dynamics, Springer-Verlag, New York, 1988.

[22] H. N. Najm, Uncertainty quantification and polynomial chaos techniques in computational fluid dynamics, Annu. Rev. Fluid. Mech. 41 (2009) 35-52.

[23] D. Xiu, J. S. Hesthaven, High-order collocation methods for differential equations with random inputs, SIAM J. Sci. Comput. 27 (2005) 1118-1139.

[24] Y. Marzouk, D. Xiu, A stochastic collocation approach to Bayesian inference in inverse problems, Commun. Comput. Phys. 6 (2009) 826-847.

[25] D. Xiu, Numerical Methods for Stochastic Computations, Princeton, New Jersey, 2010.

[26] S. Smolyak, Quadrature and interpolation formulas for tensor products of certain classes of functions, Soviet Math. Dokl. 4 (1963) 240-243.

[27] P. C. Paris, F. Erdogen, A critical analysis of crack propagation laws, J. Basic Eng. 85(1963) 528-534.

[28] J. E. Collipriest, An experimentalist's view of the surface flaw problem, The Surface Crack: Physical Problems and Computational Solutions, ASME. (1972) 43-61.

[29] K. Inoue, M. Kato, G. Deng, N. Takatsu, Fracture mechanics based of strength of carburized gear teeth, In Proceedings of the JSME International Conference on Motion and Power Transmissions. (1999) 801-806.

[30] K. Ortiz and A. S. Kiremidjian, Stochastic modeling of fatigue crack growth, Eng. Fract. Mech. 29 (1988) 317-334

[31] J. N. Yang, S. D. Manning J. L. Rudd, W. H. His, Stochastic crack propagation in fastener holes, J. Aircraft, AIAA, 22 (1985), 810-817.

[32] J. N. Yang, G. C. Salivar and C. G. Annis, Statistical modeling of fatigue-crack growth in a nickel-base superalloy, Eng. Fract. Mech. 18 (1983) 257-270.

[33] J. N. Yang, S. D. Manning, M. E. Artley, Probabilistic durability analysis methods for metallic airframes, Probabilist. Eng. Mech. 2 (1987) 9-15.

[34] C. Willhauck, S. Mohanty, A. Chattopadhyay, P. Peralta, Stochastic crack growth under variable loading for health monitoring and prognosis, in Proceedings of *SPIE* 6926, Modeling, Signal Processing, and Control for Smart Structures 2008, doi:10.1117/12.776476

[35] D. A. Virkler, B. M. Hillberry, P. K. Goel, The statistical nature of fatigue crack propagation, Air force dynamics laboratory, AFFDL-TR-43-78, 1978

[36] ASTM E647-00 *Standard Test Method for Measurement of Fatigue Crack Growth Rates*. ASTM International. 2000.

Biographies

Fuqiong Zhao is currently a Ph.D. candidate in the Department of Mechanical and Industrial Engineering at Concordia University, Canada. She received her M.S. degree in 2009 and B.S. degree in 2006 both from the School of Mathematics and System Sciences, Shandong University, China. Her research is focused on integrated prognostics, uncertainty quantification, finite element modeling and condition monitoring.

Zhigang Tian is currently an Associate Professor in the Concordia Institute for Information Systems Engineering at Concordia University, Canada. He received his Ph.D. degree in 2007 in Mechanical Engineering at the University of Alberta, Canada, and his M.S. degree in 2003 and B.S. degree in 2000 both in Mechanical Engineering at Dalian University of Technology, China. His research interests focus on reliability analysis and optimization, condition monitoring, prognostics, maintenance optimization and renewable energy systems. He received the 2011 Petro-Canada Young Innovator Award (Technology, Industry, and the Environment). He is an Associate Editor of International Journal of Performability Engineering, and serves as Vice President for the Reliability, Availability, Maintainability and Safety Professionals Society (RAMSP). He is a member of IIE and INFORMS.

Yong Zeng is a Professor in the Concordia Institute for Information Systems Engineering at Concordia University, Montreal, Canada. He is Canada Research Chair in Design Science (2004–2014). He received his B.Eng. degree in structural engineering from the Institute of Logistical Engineering and M.Sc. and Ph.D. degrees in computational mechanics from Dalian University of Technology in 1986, 1989, and 1992, respectively. He received his second Ph.D. degree in design engineering from the University of Calgary in 2001. His research is focused on the modeling and computer support of creative design activities.